

## Laser ablation for 3D nanometric imaging of solids

Ilmar Kink, Vambola Kisand, Kristjan Saal, Tanel Tätte, Madis Lobjakas,  
and Ants Lõhmus

Institute of Physics, University of Tartu, Riia 142, 51014 Tartu, Estonia; [ilmar.kink@fi.tartu.ee](mailto:ilmar.kink@fi.tartu.ee)

Received 9 October 2003, in revised form 6 November 2003

**Abstract.** A new method for subsurface nanometric imaging is proposed that combines scanning probe microscopy and laser ablation techniques. The feasibility of the method was tested on mica samples by studying laser radiation interaction with the mica surface. The ablation of the samples was characterized as functions of deposited radiation energy and of the number of laser pulses. Additional examples of applicability of the method are presented using more complex samples such as a TiC:Ni compound and a biological tooth.

**Key words:** SPM, laser ablation, three-dimensional imaging.

### 1. INTRODUCTION

Scanning probe microscopy (SPM) is now a well-established tool for precise surface analysis. Besides its superb characteristics it has a serious limitation, namely, it can reveal only limited information about subsurface properties of a sample. Its sensitivity inwards along the surface normal is severely constrained to a few topmost atomic or molecular layers. However, the subsurface region is of great interest for many applications. The surface of a sample can be easily contaminated with substances from surrounding environment and thus misrepresenting the true nature of the sample.

Currently there are only a few techniques available that are capable of spatial 3D imaging at nanometer scale and typically these are applicable only in special cases. For example, scattering techniques (X-ray, neutron, etc.) require translationally symmetric structure of the sample that is more often missing than present. Electron tomography and transmission electron microscopy can be applied for 3D imaging. However, they require complicated and time-consuming

sample preparation. The samples must be extremely thin that is not possible in many cases [<sup>1-3</sup>]. Furthermore, these techniques image primarily an electron cloud density that also limits their application. A recently developed method of magnetic resonance force microscopy is capable of real space 3D imaging of spin density that reflects the shapes and sizes of microstructures [<sup>4</sup>], however, its resolution ( $>1\ \mu\text{m}$ ) is still not comparable with SPM.

There have been attempts to employ the idea of creating a nanotomograph by stepwise removal of surface layers of a sample, taking SPM images after each removal procedure, and subsequently creating a 3D model of the sample from the images by computerized processing [<sup>5</sup>]. Despite simplicity of the idea it has turned out to be technically very challenging. The main obstacle is how to spot the same location on the sample with the SPM probe after the sample has been removed for the surface treatment procedure, or alternatively, how to protect the probe if an *in situ* removal procedure is applied. In the first case, either artificial or naturally occurring markers [<sup>5</sup>] have been used for finding the correct location for SPM imaging. However, that limits possible applications of the method. Furthermore, repeated transportation of the sample between the SPM and the processing apparatus makes the procedure time-consuming that prevents real-time applications. The second approach, where neither the sample nor the probe is removed during the surface processing, has been successfully applied in cases of selective electrochemical reactions [<sup>6</sup>] or selective chemical etching [<sup>7</sup>]. The general disadvantage of the approach is that the SPM tip is located in the vicinity of the processing area and can be modified or even destroyed.

In our previous work [<sup>8</sup>] we introduced an efficient method of scanning probe analysis and subsurface imaging that eliminates the above-mentioned technical obstacles for many practical applications. The method is based on a single integrated device, which performs pulsed laser ablation of surface layers and precise resetting of the far-removed SPM probe after ablation.

The laser ablation technique offers several advantages for controllable removal of surface layers. The laser beam is easily guided and focused on a desired region of the sample by simple optics. The ablation depth depends on the deposited energy that can be controlled by selecting appropriate parameters of laser pulses. In some cases the laser ablation does not require any additional expensive apparatus (e.g., vacuum chambers) and can be performed in ambient environment. Application of excimer lasers is quite common in pulsed laser deposition techniques [<sup>9</sup>] because the excimer lasers offer sufficient energy density ( $>1\ \text{J}/\text{cm}^2$ ) and their lasing transitions typically occur in the suitable wavelength range of 150–400 nm where most materials have strong absorption bands and correspondingly small penetration depths.

## 2. EXPERIMENTAL SET-UP

The experimental set-up (Fig. 1) consists of a SPM (Smena-B, NT-MDT, Russia), UV excimer laser (PSX-100, Neweks, Estonia), quartz optics for directing

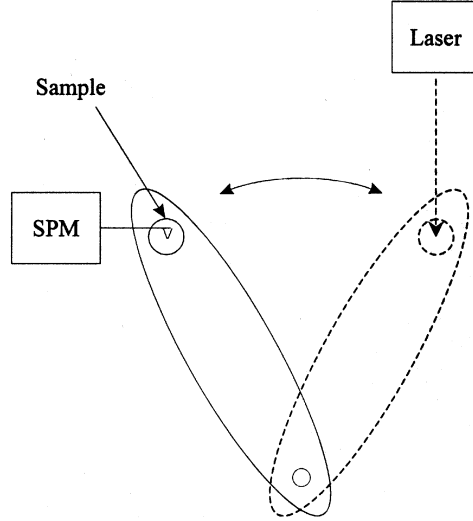


**Fig. 1.** Layout of the mechanics of the experimental set-up.

the laser beam onto the sample, and a computer-controlled translation mechanism for separating the sample and the AFM probe for the ablation process. The precision of the latter is critical for subsequent comparison of the images and creating a 3D model of the sample. The accuracy can be vastly improved by using naturally occurring markers for correcting mechanical shifts. However, the precision of mechanical movements should be at least higher than the scan dimensions; otherwise the method becomes prohibitively inefficient. When markers cannot be defined, the mechanical accuracy constrains applicability of the method setting lower limits on the dimensions of the structures that can be imaged. However, typically the surface structures of the samples are characteristic enough to be used as markers and thus they significantly improve the overall usability of the method. The mechanical misalignment of the device is  $100 \pm 30$  nm where the error represents statistical accuracy of 15 test measurements. The compensating shifts can improve the accuracy by a factor of 4. The latter value was obtained by using one marker for shifting the images and relative positions of other markers as indicators of the accuracy of the shifts.

The laser was typically operating at 193 nm wavelength (ArF), 3 mJ average pulse energy, 5 ns pulse duration, 0–10 Hz repetition rate. The laser beam was focused onto a target by a  $f = 210$  mm quartz lens. Typical dimensions of the beam were 200–300  $\mu\text{m}$  that is more than one order of magnitude larger than typical scan dimensions (1–10  $\mu\text{m}$ ). Therefore the laser radiation within the scan area can be assumed homogeneous except in special cases (see next section).

All experiments were performed in ambient environment.

### 3. METHOD AND RESULTS

#### 3.1. Method in general

It is widely known that laser ablation mechanism of solid surfaces is a complicated phenomenon consisting of several competing processes. Detailed model of the removal of the material from surfaces is less adequate in case of dielectric films as compared to metals because in the former case the optical and thermal absorption depths are of the same order of magnitude. Several irregularities on modified surfaces have frequently been observed. For instance, it has been shown [10] that the laser irradiation can produce several different surface modification patterns (periodic ripples, cones, etc.) depending on the deposited energy and laser beam properties. Also, different substances have different removal thresholds [11], and ablation properties depend on the deposited energy. If relevant, these phenomena may seriously hamper application of the SPM tomography for the determination of the internal nanostructure of objects because ablation-created structures are generally indistinguishable from the real ones.

For general investigation of the relevance of the ablation effects in SPM tomography, a series of different test samples was prepared and studied. The results indicate that in all cases it was possible to select laser parameters so that significant ablation effects, which could critically restrict SPM tomographic method, were not observed. Typically, significantly shorter irradiation times were used as compared to other investigations where these phenomena were observed. For example, in the case of gold-coated silicon samples at significantly longer exposition times ( $>1000$  pulses instead of typical 1–20 pulses) we saw patterns similar to hydrodynamic sputtering [12], observed by Kelly et al. [13].

#### 3.2. Nanoablation of mica

Mica is a convenient target surface for testing the SPM tomographic method because its atomic scale flatness is suitable for imaging with an AFM being thus also extensively used as a support for AFM measurements of various objects. On the other hand, large-scale UV laser radiation effects on the mica surface have also been studied [14]. These studies were partially motivated by sweeping technological applications of mica, improving reliability of the data by comparing results of the complementary techniques.

In our experiments we used freshly cleaved surface of commercially supplied mica (Proscitech, Australia).

Three different kinds of energy dependence can be distinguished. At energy densities above the ablation threshold but lower than  $5 \text{ mJ/mm}^2$ , the surface structures of a sample remain virtually unchanged. However, infrequently the laser radiation causes appearance of very sharp steps on the surface. It is conceivable that the material “flies off” uniformly layer by layer in relatively large ( $>>500 \text{ }\mu\text{m}^2$ ) pieces leaving cavities with very sharp edges on the surface (Fig. 2). It is likely that the edge appears in the border region of the laser spot

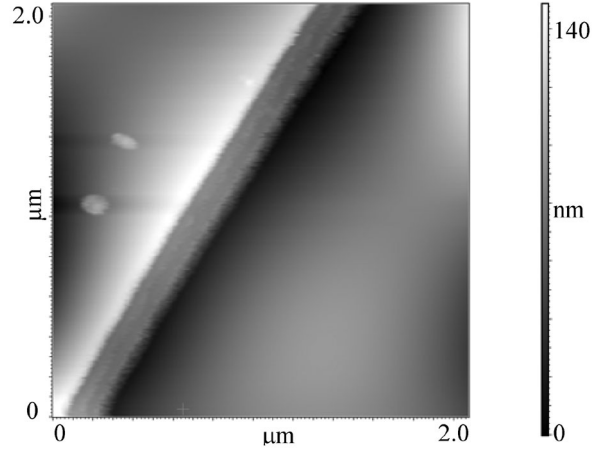


**Fig. 2.** Mica surface after interaction with low fluence ( $<5 \text{ mJ/mm}^2$ ) UV laser (193 nm) radiation; a border area between interacting and non-interacting regions is shown; note that interacting region remains atomically flat that is generally characteristic for mica surface, that is, no atomic-scale structural modifications have been caused by the photon interaction.

where the radiation intensity begins to fall. However, large uncertainties in laser spot location make it difficult to prove.

In the “high” energy density region ( $\geq 300 \text{ mJ/mm}^2$ ), the amount of abruptly absorbed radiation energy is large enough to destroy crystallographic structure in near-surface regions, causing besides removing a fraction of the material also “boiling” in the below-surface region. That results in chaotic and large structures (Fig. 3), which do not resemble the original surface. These structures are supposedly “seeds” for larger regular structures, frequently observed in laser ablation processes [14]. However, experimental verification is related to some technical challenges because further increase of the laser energy would result in structures larger than the “vertical” (z axis) range of the SPM.

A characteristic property of the intermittent region between the two extremes is the presence of small randomly distributed structures (Fig. 4). The general rule is that the density of the structures increases with energy. The in-plane shapes of the structures vary significantly whereas vertical dimensions remain constant ( $6.1 \text{ \AA}$ ) within experimental uncertainties. Note that the distance between equivalent crystallographic planes in mica is  $12.9 \text{ \AA}$  [14]. Energy dependence of the formation of the structures was very complicated and non-linear. Minor changes of some laser parameters can result in drastic changes of surface structures. Moreover, we have frequently observed peculiar inconsistencies in the shape of the structures, explanation of which needs further investigation. It is plausible that there are several different mechanisms (e.g., selective and inhomogeneous ablation, debris of the back-fallen material, nanoscopic evaporation centres below the surface, etc.)

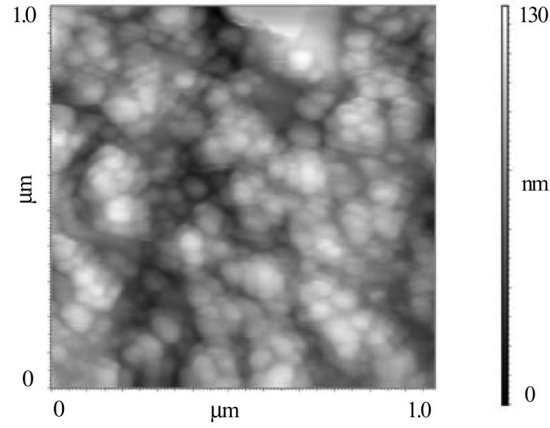


**Fig. 3.** Mica surface after interaction with high fluence ( $>300 \text{ mJ/mm}^2$ ) UV laser (193 nm) radiation, where strongly modified “boiled” surface is seen.

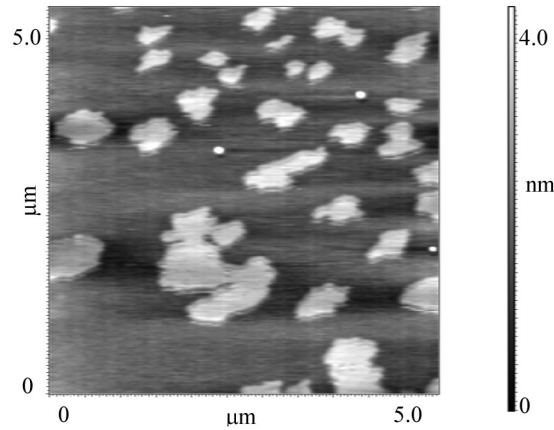


**Fig. 4.** Mica surface after interaction with intermittent fluence ( $5\text{--}300 \text{ mJ/mm}^2$ ) UV laser (193 nm) radiation; modified surface structures and back-fallen debris of ablated material are seen.

causing the structures, interplay of which results in their seemingly chaotic and inconsistent formation.

It is obvious that only the low-fluence regime can be suitable for SPM tomography because no indistinguishable structural changes are caused by the laser radiation. The laser-induced structures in other regimes are easily confused with real subsurface structures of complex samples, leading to erroneous 3D models of the samples.

Currently one of the problems, slowing the implementation of the SPM tomographic method, is vertical calibration, that is, uncertainty in determination of the “distance” between two subsequent SPM images taken before and after laser ablation. The formation of the sharp edge during low-fluence laser ablation can significantly improve 3D modelling of a sample providing clear set point for vertical calibration. Without it one has to rely on other methods that all have more or less serious limitations. For example, one can employ the fact that materials have different ablation thresholds and use non-ablative artificial or natural markers. A universal method is to mask partially the ablation region and use non-ablated region as the set point. It is also possible to use indirect methods, e.g., to measure the mass loss of the sample, etc.

### 3.3. Other examples

One of the appealing applications of SPM tomography is the possibility to determine internal structure of complex multi-component materials like compounds, biological structures, artificial nanostructures, etc. As test objects we have selected TiC:Ni samples and a biological tooth. The selection is partly motivated by some aspects of our other research projects. Figure 5 shows preliminary test images of the samples indicating that the method can be used also in the cases of complicated complex structures. It is still an ongoing investigation, nevertheless, already now we have monitored selective ablation processes of the complex surfaces. Generally, softer materials (e.g., Ni in the case of the TiC:Ni compound) tend to be ablated more easily; however, the optimum conditions are yet to be determined. Therefore the detailed analysis of the structures in Fig. 5 can be misleading and the figure serves only an illustrative purpose showing which type of objects we expect to analyse using the SPM tomography.

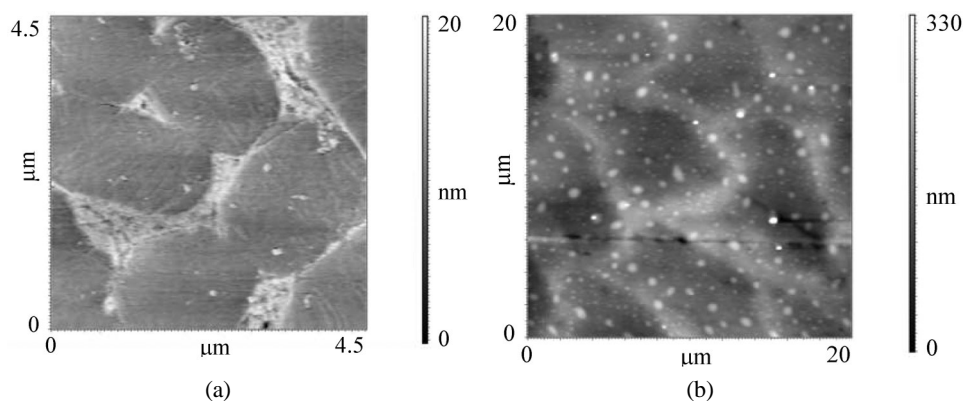


**Fig. 5.** Illustrative examples of complex objects that are expected to be studied in detail using SPM tomography: (a) phase image of TiC:Ni where TiC particles (dark ovals) and Ni particles are easily distinguished; (b) topographic image showing complicated inner structure of a human tooth.

#### 4. CONCLUSIONS

As the first step towards development of the SPM tomographic method it was shown that UV laser ablation can be utilized. It was shown that in the case of mica the laser fluences below  $5 \text{ mJ/mm}^2$  ( $\lambda = 193 \text{ nm}$ ) are suitable for the method. Furthermore, formation of a sharp edge during the ablation procedure is proposed for “vertical” calibration set point in further development of the method. Future plans involve investigation of complex samples possessing nanoscale internal structures. In parallel, the experimental set-up will be modified enabling accurate z-scale calibration and laser ablation processing in vacuum. The latter is mainly expected to clarify some issues related to the influence of back-fallen debris. Alternative ablation methods (mechanical and chemical) will be considered as potentially complementary techniques in specific cases.

#### ACKNOWLEDGEMENTS

We thank Dr. I. Hussainova from the Tallinn Technical University for providing TiC:Ni samples. This work was supported by Estonian Science Foundation (grant No. 5545). Support of EC FW5 “Centres of Excellence” programme (ICA1-1999-70086) is gratefully acknowledged.

#### REFERENCES

1. Sjöstrand, F. S. Ultrastructure of retinal rod synapses of the guinea pig eye as revealed by three-dimensional reconstruction from serial sections. *J. Ultrastruct. Res.*, 1958, **2**, 122–170.
2. Gaunt, W. A. and Gaunt, P. N. *Three Dimensional Reconstruction in Biology*. Pitman Medical, Kent, 1978.
3. Frank, J. *Three-dimensional Electron Microscopy of Macromolecular Assemblies*. Academic Press, San Diego, 1996.
4. Wago, K., Botkin, D., Yannoni, C. S., and Rugar, D. Paramagnetic and ferromagnetic resonance imaging with a tip-on-cantilever magnetic resonance force microscope. *Appl. Phys. Lett.*, 1998, **72**, 2757–2759.
5. Magerle, R. Nanotomography. *Phys. Rev. Lett.*, 2000, **85**, 2749–2752.
6. Siebel, E. M., Memmert, U., Vogel, R., and Hartmann, U. A scanning force microscope for *in situ* observation of electrochemical processes. *Appl. Phys. A*, 1998, **66**, S83–S86.
7. Bukharev, A. A., Nurgazizov, N. I., Ovchinnikov, D. V., and Mozhanova, A. A. *In situ* investigation of chemical etching of implanted silicon dioxide in aqueous solutions by atomic-force microscopy. *Russian J. Appl. Chem.*, 2000, **73**, 1332–1338.
8. Kink, I. et al. Three-dimensional subsurface imaging with laser ablation/AFM. In *Advanced Optical Devices, Technologies and Medical Applications* (Spigulis, J. et al., eds.). *Proc. SPIE*, 2003, **5123**, 266–269.
9. Green, S. M., Piqué, A., Harshavardhan, K. S., and Bernstein, J. Equipment. In *Pulsed Laser Deposition of Thin Films* (Chrisey, D. B. and Hubler, G. K., eds.). Wiley, New York, 1994, 23–25.
10. Van Driel, H. M., Sipe, J. E., and Young, J. F. Laser-induced periodic surface structure on solids: A universal phenomenon. *Phys. Rev. Lett.*, 1982, **49**, 1955–1958.



11. Walkup, R. E., Jasinski, J. M., and Dreyfus, R. W. Studies of excimer laser ablation of solids using a Michelson interferometer. *Appl. Phys. Lett.*, 1986, **48**, 1690–1692.
12. Kelly, R. and Miotello, A. Mechanisms of pulsed laser sputtering. In *Pulsed Laser Deposition of Thin Films* (Chrissey, D. B. and Hubler, G. K., eds.) Wiley, New York, 1994, 55–88.
13. Kelly, R. et al. Laser sputtering, Part I: On the existence of rapid laser sputtering at 193 nm. *Nucl. Instrum. Meth. Phys. Res.*, 1985, **B9**, 329–340.
14. Rubahn, K., Ihelmann, J., and Rubahn, H. G. Excimer laser sputtering of mica surfaces: Mechanisms and applications. *J. Appl. Phys.*, 1999, **86**, 2847–2855.

## **Tahkise ruumilise struktuuri nanomeetriline kujutamine laserablatsiooni abil**

Ilmar Kink, Vambola Kisand, Kristjan Saal, Tanel Tätte, Madis Lobjakas  
ja Ants Lõhmus

Artiklis kirjeldatakse uut, kombineeritud meetodit tahkise pinnaaluse ruumilise struktuuri nanomeetrilise täpsusega kujutamiseks, mis ühendab endas skaneeriva teravikmikroskoopia ja laserablatsiooni eksperimenditehnikad. Meetodit rakendati ultraviolettkiirguse mõju uurimisel vilgu pinnale. Tuvastati seosed nanoskoopiliste pinnamoonutuste tekkimise ja neeldunud kiirgusdoosi ning laserimpulsside arvu vahel. Lisaks on toodud kaks näidet keerulisematest objektidest, mille uurimiseks kavatakse kirjeldatud meetodit tulevikus rakendada.